J. Fluid Mech. (1995), vol. 297, pp. 357–372

Hydrodynamical instabilities of thermocapillary flow in a half-zone

By MÅRTEN LEVENSTAM† AND GUSTAV AMBERG
Department of Mechanics, Royal Institute of Technology, S-100 44 Stockholm, Sweden

(Received 21 February 1994 and in revised form 14 February 1995)

The stability of the flow in a half-zone configuration is analysed with the aid of direct numerical simulation. The work is concentrated on the small Prandtl numbers relevant for typical semiconductor melts. The axisymmetric thermocapillary flow is found to be unstable to a steady non-axisymmetric state with azimuthal wavenumber 2, for a zone with aspect ratio 1. The critical Reynolds number for this bifurcation is 1960. This three dimensional steady solution loses stability to an oscillatory state at a Reynolds number of 6250. For small Prandtl numbers, both bifurcations are seen to be quite insensitive to changes in the Prandtl number, and are thus hydrodynamic in nature. An analogy to the instability of thin vortex rings is made. This analogy suggests a physical mechanism behind the instability and also gives an explanation of how the azimuthal wavenumber of the bifurcated solution is selected. The implications of this for the floating-zone crystal growth process are discussed.

1. Introduction

One method for the production of single crystals of semiconductors is the so-called float-zone method (FZ). In this method a drop of semiconductor melt is held by surface tension forces between two solid rods of the same material. The drop is kept molten by an intense heat source focused on it. The two suspending rods are cooled, and the heat source is passed slowly along the rod so that the material melts and re-solidifies as the heat source passes. After one or several such passes the purity and the crystal structure of the rod is greatly improved. The main advantage of this method is that it is containerless, and thus makes it possible to produce extremely pure crystals.

It has long been known that the fluid motion in this system is caused both by gravitational and thermocapillary convection. The convection has undesired effects and as a means of suppressing the gravitational convection, the FZ-method has been proposed for space processing of materials. However, owing to the intense temperature gradients that are present over the drop surface, the thermocapillary convection may be significant, even on Earth. A lot of attention has been focused on the thermocapillary convection in this system. One of the first works to point out the importance of thermocapillary effects was Chang & Wilcox (1976).

Experiments on the FZ method, both on Earth and in microgravity conditions in space, have shown a banded structure, striations, in the chemical composition of the finished crystals. From this it has been suggested that the flow in the FZ has been

† Present adress: Department of Mathematics, Chalmers University of Technology, S-411 22 Göteborg, Sweden.

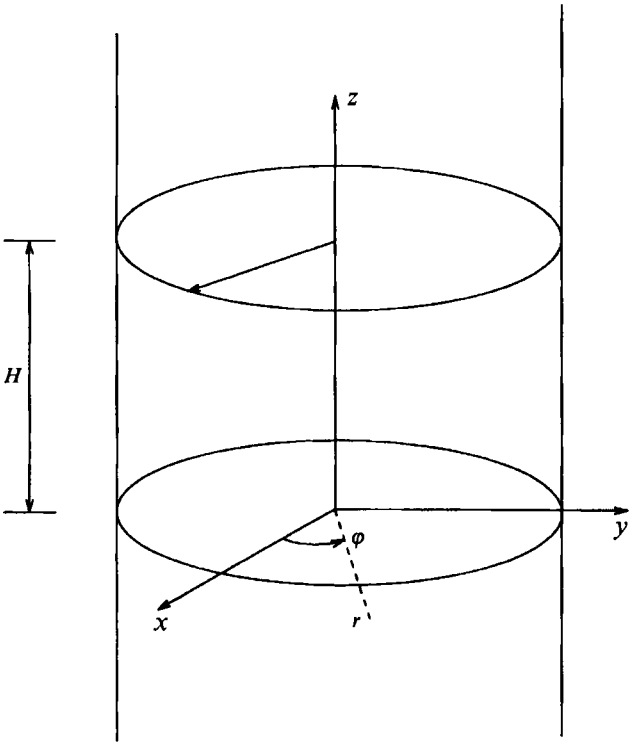

FIGURE 1. The geometry of the half-zone.

oscillatory in time during the growth of the crystal. These striations are undesirable and actually limit the usefulness of the FZ-method. The flow oscillations are believed to be the result of an instability of the steady thermocapillary convection causing a flow which is periodic in time. It is hoped that a thorough understanding of this phenomenon could suggest ways to improve the design of the crystal growth process. This problem has also attracted attention recently as a representative of a class of basic stability problems of thermocapillary convection.

Much of the recent work in this area has been done on a simpler model problem, the half-zone (HZ). In this problem the heat source is replaced by maintaining different temperatures on the two suspending rods, see figure 1. A number of experiments with this system has been carried out for different liquids. All these liquids had higher Prandtl numbers than those typical of semiconductor melts. The typical result of these experiments is that there is a transition from steady axisymmetric flow to oscillatory three dimensional flow at some critical point. In the work of Preisser, Schwabe & Scharmann (1983) detailed experiments are carried out to detect the critical points for the onset of oscillatory flow and flow visualizations to identify the spatial structure of the bifurcated solutions.

The transition from steady to oscillatory thermocapillary convection has been studied theoretically by several authors, in different geometries. Several distinct instability mechanisms leading to oscillatory flow have been demonstrated. One is the surface wave instability described by Smith & Davis (1983*b*), which is caused by the interaction of the base-state shear at the interface, and the velocity disturbance induced by a perturbation of the free surface. Thermocapillarity is thus important

only for maintaining the base state for this mechanism. This instability has also been found in two numerical studies in both two-dimensional containers and axially symmetric floating zone configurations, Kazarinoff & Wilkowski (1989, 1990).

Thermocapillarity is however crucial in producing the hydrothermal waves of Smith & Davis (1983*a*) and Smith (1988). The underlying mechanisms, which have been described by Smith (1986), are different for low and high Prandtl numbers, as well as for different base-state velocity profiles (notably linear for Couette flow in a two-dimensional layer, parabolic for return flow with no net volume flux along the layer). The ones that are most relevant to the present study are the hydrothermal waves for return flow, which exhibit rolls propagating approximately perpendicularly to the surface flow for $Pr < 1$, and approximately two-dimensional rolls propagating against the direction of the surface flow for $Pr > 1$, Smith (1986) and Smith & Davis (1983*a*). This type of instability has also been found in infinitely long cylindrical liquid rods, Xu & Davies (1983, 1984).

In two-dimensional containers of finite length, thermocapillary-driven flow may exhibit a steady spanwise roll structure, Ben Hadid & Roux (1990), and Villers & Platten (1992). At a Prandtl number around 4, these rolls have been observed to become oscillatory when the forcing is increased, Villers & Platten (1992), and may be related to the large Prandtl number instability mechanism of Smith (1986). However, at least for small Prandtl numbers, the instability leading to the appearance of the steady pattern seems to be entirely hydrodynamical. This is suggested by the fact that the patterns did appear in the simulations by Ben Hadid & Roux (1990), even though the temperature and velocity fields were decoupled in most of their runs.

To the authors' knowledge, the only three-dimensional direct numerical simulation of the HZ that has been reported in the literature is that by Rupp, Müller & Neumann (1989). They studied both small and large Prandtl numbers, and noted that for small Prandtl numbers the time-dependent flow is preceded by a bifurcation to a steady non-axisymmetric state. No critical numbers for this bifurcation are presented, however. There is only one result presented for this steady non-axisymmetric flow which at those parameter values is a solution with an azimuthal wavenumber of 2. Furthermore the numerical resolution was limited and no assessment of the accuracy of the numerical solutions was reported.

Energy stability methods have been used by Shen *et al.* (1990) and Neitzel *et al.* (1991) to study the stability of the flow in a HZ. In both these works the basic state is computed numerically and the stability analysis is performed on this state. In the first paper axially symmetric disturbances were considered for a range of Prandtl numbers. In the second, the disturbances were allowed to be three-dimensional while the Prandtl number was fixed at $Pr = 1$ and the aspect ratio of the HZ was varied.

Linear stability analysis of the HZ problem has been performed by Neitzel *etl al.* (1993). In this work the basic state is computed numerically and the linear stability problem is solved for three-dimensional disturbances. The Prandtl number is fixed at 1 and the aspect ratio is varied. For this Prandtl number they find a time-periodic instability with an azimuthal wavenumber of 2.

Another linear stability analysis has been done by Kuhlmann & Rath (1993). In this work the aspect ratio of the zone is fixed at 1 and a span of Prandtl numbers are investigated. The basic state is computed numerically. These basic states are limited to axisymmetric states but the stability analysis allows for three-dimensional disturbances. For small Prandtl numbers the first bifurcation from an axisymmetric state was found to be to a steady non-axisymmetric state. The critical eigenmode

for this instability is found to have an azimuthal wavenumber of 1. This instability remains for very small Prandtl numbers indicating that it is purely hydrodynamical in character. Since the method used in that work is unable to treat non-axisymmetric basic states no results for the bifurcation to time-periodic flow are computed for small Prandtl numbers. For larger Prandtl numbers the results in Kuhlmann & Rath (1993) indicate a hydrothermal instability of the type described in Smith & Davis (1983*a*) with an azimuthal wavenumber of 1.

As shall be evident from the later sections of this paper our results do not agree with those of Kuhlmann & Rath (1993). Apparently there was some error in their calculations, which was discovered after the publication of their paper (Kuhlmann, private communication 1994). They have since repeated some computations, and did then get results which are in agreement with our results and those of Rupp *et al* (1989).

In the present work the nonlinear evolution of the flow in a HZ is studied as the Reynolds number is increased. In order to focus on the technically important case of semiconductor melts, the work is concentrated on small and zero Prandtl numbers. The first instability is shown to be a hydrodynamical instability with many similarities to that for thin vortex rings. This analogy gives an indication of why the flow becomes unstable, and how the azimuthal wavenumber of the bifurcated solution is selected. As the Reynolds number of the flow increases, this steady three-dimensional state bifurcates into a periodic time-dependent flow. This transition is also shown to be a purely hydrodynamical instability. Conditions for this transition and properties of the flow are given.

The paper is organized as follows. In § 2 the mathematical model of the HZ is presented. In § 3 a short description of the numerical method is presented. The results of the computations together with a discussion of the instabilities are given in § 4.

2. Mathematical model

The half-zone consists of a cylindrical liquid bridge hanging between two circular flat interfaces, see figure 1. The liquid is kept in place by surface tension forces acting on the free surface. The distance between the flat interfaces is H and the radius is R. A temperature difference is maintained over the liquid bridge by prescribing T_{bottom} and T_{top} at the bottom and top interfaces respectively. In the following we will assume that $T_{bottom} > T_{top}$, and we will frequently refer to the bottom and top faces as 'hot' and 'cold' respectively.

The surface tension, acting on the free surface, is considered to be a linearly decreasing function of temperature,

$$\Gamma = \Gamma_0 - \gamma T. \tag{2.1}$$

This dependency together with the temperature gradient on the free surface will drive a motion in the liquid bridge. The constant γ is assumed to be positive, which means that the surface stress will generally tend to pull away from a high-temperature spot on the surface. The equilibrium shape of the the free surface is determined by the net surface tension, which is assumed so large (i.e. very small capillary number) that the interface assumes a perfectly cylindrical shape.

The fluid in the zone is treated as an incompressible Newtonian liquid. The equations governing the fluid's motion and temperature are thus the incompressible

Navier–Stokes equations and the energy equation. They are given in non-dimensional form by:

$$\frac{\partial \boldsymbol{u}}{\partial t} + \boldsymbol{u}\nabla\cdot\boldsymbol{u} = -\nabla p + \frac{1}{Re}\nabla^2\boldsymbol{u}, \tag{2.2}$$

$$\nabla\cdot\boldsymbol{u} = 0, \tag{2.3}$$

$$\frac{\partial T}{\partial t} + \boldsymbol{u}\nabla\cdot T = \frac{1}{RePr}\nabla^2 T. \tag{2.4}$$

They are to be solved together with the boundary conditions:

$$\boldsymbol{u}\cdot\boldsymbol{n} = 0, \quad r = A, \tag{2.5}$$

$$S_{ij}n_j - n_i(n_k S_{kj} n_j) = -\left(\frac{\partial T}{\partial x_i} - \left(\frac{\partial T}{\partial x_i}n_i\right)n_j\right), \quad r = A, \tag{2.6}$$

where S_{ij} is the stress tensor.

$$\nabla T\cdot\boldsymbol{n} = 0, \quad r = A, \tag{2.7}$$

$$\boldsymbol{u} = \boldsymbol{0}, \quad T = 1, \quad z = 0, \tag{2.8}$$

$$\boldsymbol{u} = \boldsymbol{0}, \quad T = 0, \quad z = 1. \tag{2.9}$$

The equations (2.6) can be found from a stress balance at the free surface. It is also, from these equations, obvious that as soon as there is a temperature gradient across the free surface there is also a motion set up in the zone.

These equations have been made non-dimensional using the height of the zone as a typical length and the following scales for velocity, temperature and time:

$$U = \frac{\gamma\Delta T}{\mu}, \tag{2.10}$$

$$\Delta T = T_{top} - T_{bottom}, \tag{2.11}$$

$$\tau = H/U. \tag{2.12}$$

The non-dimensional numbers appearing in the equations are the Reynolds number, Re, the Prandtl number, Pr, and the aspect ratio, A. They are defined as

$$Re = \frac{\gamma\Delta T H}{\mu\nu}, \tag{2.13}$$

$$Pr = \frac{\nu}{\kappa}, \tag{2.14}$$

$$A = \frac{R}{H}, \tag{2.15}$$

where μ and ν are the dynamical and kinematical viscosities, κ is the thermal diffusivity. Often the Marangoni number, $Ma = \gamma\Delta T H/\mu\kappa = RePr$, is used instead of the Reynolds number. It should be noted here that the velocity scale is somewhat arbitrary. Zebib, Homsy & Meiburg (1985) showed that the magnitude of the velocity is much smaller than the reference velocity used above, and that the corresponding Reynolds number thus overestimates the importance of inertia relative to viscous forces.

3. Numerical method

A finite element method with tri-quadratic isoparametric interpolation for velocity, pressure and temperature, giving a predicted third-order-accurate method, has been

Grid ($n_r \times n_\varphi \times n_z$)	U_{max}	U_φ
$10 \times 16 \times 10$	0.08876	0.0115
$20 \times 16 \times 20$	0.08872	0.0130
$20 \times 32 \times 20$	0.08671	0.0132
$30 \times 48 \times 30$	0.08647	0.0134

TABLE 1. Results on different grids, $Re = 3500$, $Pr = 0.01$.

used. The restrictions imposed by the Babushka-Brezzi condition are avoided by using a method similar to that by Hansbo & Szepessy (1990). The time discretization is done using an Euler implicit scheme for the viscous terms and an Euler explicit scheme for the nonlinear advection terms. The pressure is decoupled from the velocity computations by using a projection method as described in Shien (1993).

This method requires the solution of linear systems of equations at each time step. These systems are symmetric and positive definite and are solved efficiently with the conjugate gradient method using an incomplete Cholesky decomposition as a preconditioner, Golub & van Loan (1989).

3.1. *Validation*

Great care has been taken in the verification of the computer code. We have checked our nonlinear computations against those in a two-dimensional box with thermocapillary convection, Zebib *et al.* (1985), with excellent agreement. An axisymmetric HZ solution (Shen *et al.* 1990) was also computed for the actual geometry used in the present study, i.e. a cylinder. To validate the azimuthal component of the thermocapillary boundary conditions, the flow in an annular region where the shear stress is prescribed on the outer surface was computed and compared with the analytical solution for this problem.

To check the influence of the grid resolution, a bifurcated flow field was computed on several different grids for $Re = 3500, Pr = 0.01$, as presented in table 1. The maximum velocity and the maximum azimuthal velocity can be seen in table 1 as a function of the number of grid points in the r-, φ- and z-directions, respectively. The accuracy of the bifurcated solution is better than 3% on the $20 \times 16 \times 20$ mesh.

Solutions have been traced through increasing values of the Reynolds number. An available solution at a lower Reynolds number has been used as initial condition and the flow has been simulated time dependently until it has been judged to be either steady or periodic. For the time-periodic regimes the Reynolds number has been both increased and decreased in order to check for any hysteresis.

4. Results

4.1. *Basic state*

For sufficiently weak axial temperature gradients, i.e. low Reynolds numbers, the thermocapillary convection in a HZ is steady and axisymmetric. This parameter range has been studied in numerous previous works, see Chang & Wilcox (1976). The flow field can be characterized as a single axisymmetric toroidal vortex. The orientation of the vortex is such that the flow on the free cylindrical surface is directed from the hot end of the zone, towards the cold end, if surface tension decreases with temperature. For small Prandtl numbers and Reynolds numbers small

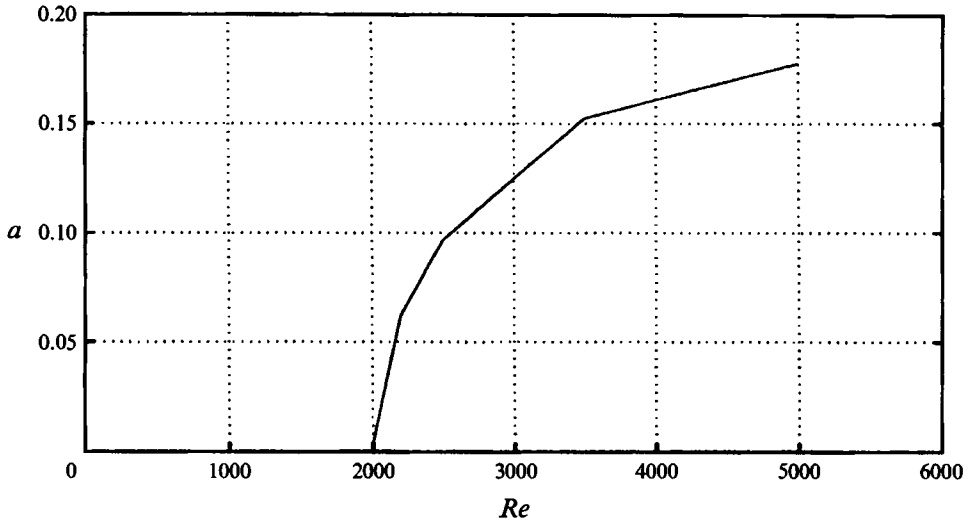

FIGURE 2. Amplitude of the bifurcated solution, $Pr = 0.01, A = 1$.

enough for the flow to be steady and axisymmetric, the effect of convection on the temperature field is insignificant (a properly defined Péclet number is small).

4.2. *The first bifurcation: steady three-dimensional state*

The steady axisymmetric solution described above persists up to a Reynolds number of $Re = 1960$ at a Prandtl number of $Pr = 0.01$. At that value of Re, the axisymmetric state described in the previous section bifurcates into a three-dimensional steady state with an azimuthal wavenumber of 2. The amplitude of the bifurcated solution, as obtained from the nonlinear computations, can be seen in figure 2. Here the amplitude has been defined as the magnitude of the azimuthal flow compared to the maximum axial velocity in the zone. Close to the critical point the amplitude is proportional to $(Re - Re_c)^{1/2}$ as expected for a supercritical bifurcation. In the three-dimensional supercritical state, the azimuthal velocity is non-zero. As Re increases, it quickly grows to be of a significant magnitude. At $Re = 3500$, the amplitude of the azimuthal flow is close to 15 % of the maximum velocity in the zone.

The nonlinear supercritical solution for $Re = 3500, Pr = 0.01$, is shown in figures 3–5. In figure 3 the velocity field can be seen in a horizontal cut at $z = 0.5$. Figures 4 and 5 show the velocity field in two orthogonal vertical cuts at $\varphi = 0$ and $\varphi = \pi/2$, through a diameter of the zone. It is seen that the core of the vortex has moved up and out, i.e. towards the free surface and towards the cold interface in the cut at $\varphi = 0$. In the cut at $\varphi = \pi/2$, the vortex centre has moved in the opposite direction, away from the free surface and towards the hot interface.

The associated temperature field can be seen in corresponding cuts in the same figures. The influence of convection on the temperature field is still weak but the azimuthal flow has produced two hot and two cold spots on the free surface.

It is of interest to note that the flow on the free surface is towards the hot spots and away from the cold spots. This is in contrast to what would be expected from the thermocapillary effect which would produce flow away from hot spots and towards cold spots. Thus the thermocapillary effect here acts as a weak force counteracting the azimuthal flow.

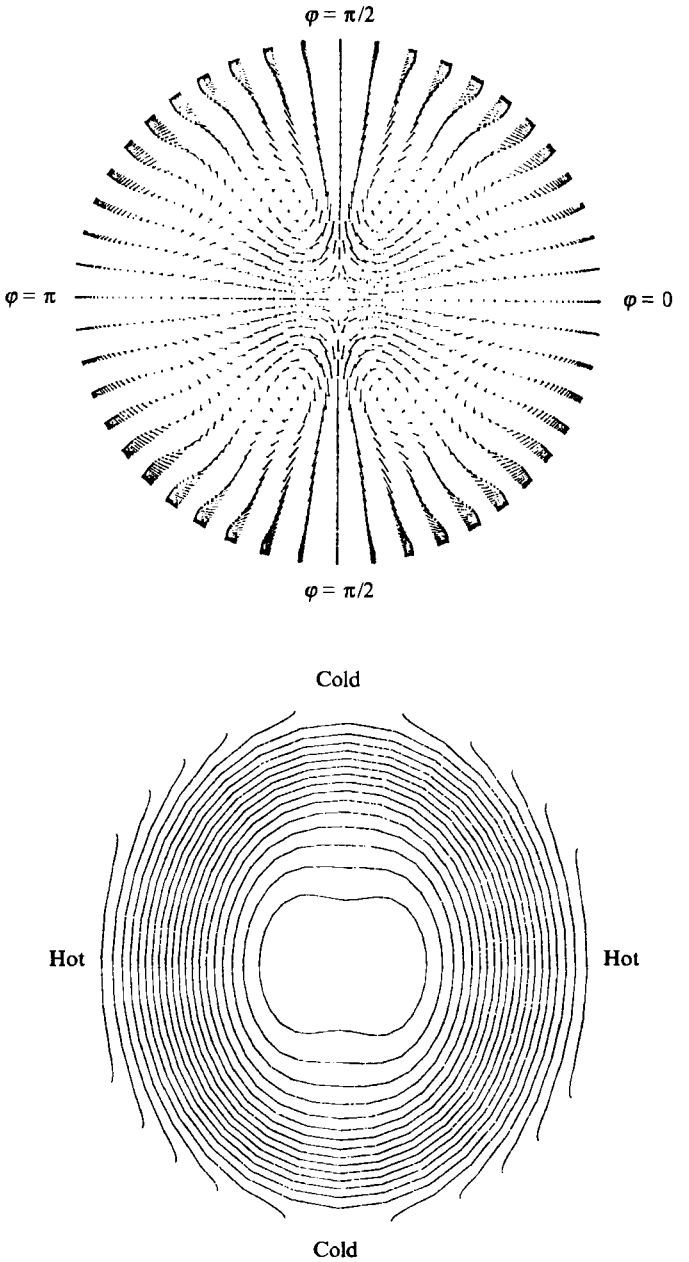

FIGURE 3. Velocity and temperature field at $z = 0.5$, $Re = 3500, Pr = 0.01$. Isotherms from 0.45 to 0.55, increment 0.005.

This indicates that the transition from steady, symmetric flow to steady, three-dimensional flow is caused by a purely hydrodynamical effect. In other words, the role of the surface tension variation is only to drive the base flow. The loss of stability at $Re = 1960$ occurs because this basic flow pattern becomes unstable in the interior; the coupling between temperature and velocity at the surface is not important for the instability mechanism. To check this conjecture, a case similar to that described

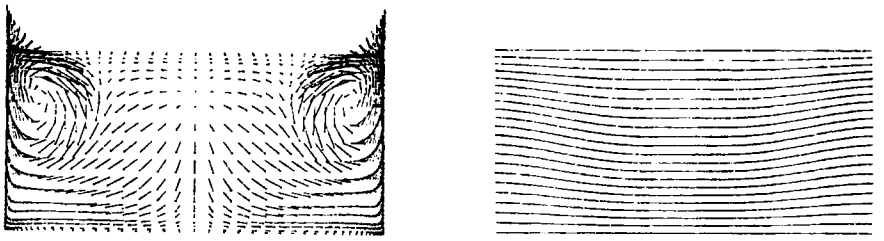

FIGURE 4. Velocity and temperature field at $\varphi = 0, \pi$, $Re = 3500, Pr = 0.01$. Isotherms from 0 to 1, increment 0.05.

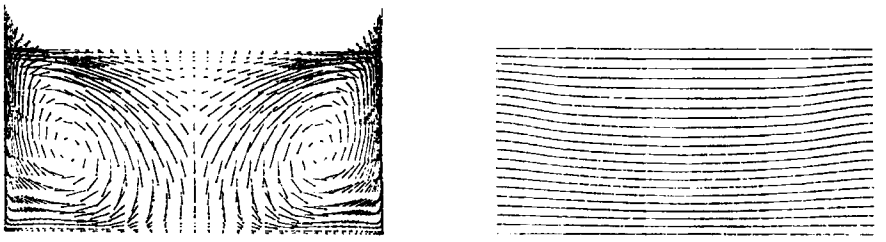

FIGURE 5. Velocity and temperature field at $\varphi = \pm\pi/2$, $Re = 3500, Pr = 0.01$. Isotherms from 0 to 1, increment 0.05.

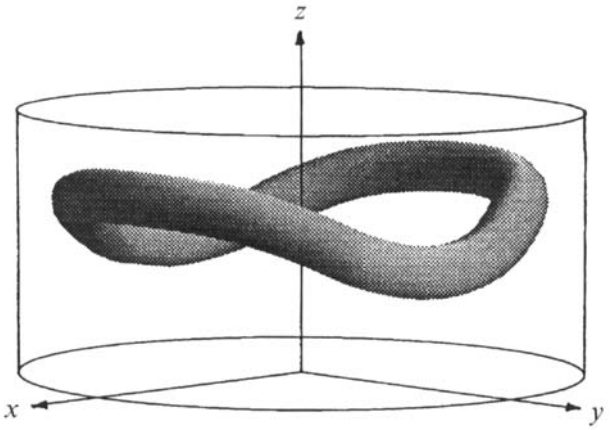

FIGURE 6. Position of the vortex core, $Re = 3500, Pr = 0.01$.

above was computed, with the only difference that the Prandtl number was set to zero. The same type of instability appeared in this case at $Re = 1898$. This shows clearly that the first bifurcation is not caused by a thermocapillary effect.

To understand the mechanism behind this instability it is instructive to take a closer look at the bifurcated solution. In figure 6 the position of the vortex core in the bifurcated solution can be seen. The figure shows the location of the vortex core with an arbitrary thickness added. In the axisymmetric basic state this would simply be an axisymmetric toroid. In the bifurcated solution the vortex core is, as can be seen in figure 6, saddle shaped.

This saddle-shaped vortex shares many properties with the solution obtained for unstable vortex rings. In the work by Widnall & Tsai (1977) the stability of a thin

vortex ring with constant vorticity in the core is analysed. They find that a vortex ring is almost always unstable. The instability is caused by the local straining motion that a curved vortex filament induces on itself. This effect is present in the HZ problem as well, but the presence of sidewalls and the free surface makes it difficult to make an exact analogy between the two problems. However, as we will see, there are striking similarities which makes us inclined to believe that the basic instability mechanism is the same.

This theory for the stability of thin vortex rings predicts that the position of the vortex after the bifurcation will be displaced sinusoidally along the perimeter of the vortex core. The vortex will be displaced both vertically and radially along lines inclined at an angle of 45° with respect to the vertical axis. The orientation of these lines is such that the part of the vortex that is displaced towards the centre is also displaced downwards and correspondingly the part of the vortex that is displaced away from the centre is at the same time displaced upwards (for a vortex ring with the same orientation as the base flow in the HZ). The growth rate is real, so the disturbance is predicted to grow exponentially in time.

The steady solution in the HZ can be viewed as having experienced an instability which has grown until is has saturated nonlinearly. The fact that the nonlinear solution is steady instead of oscillatory indicates that the linear growth rate would be real instead of complex, in agreement with the theory for thin vortex rings. Also, for the HZ, as seen in figures 4–6 , the displacement of the vortex core is qualitatively similar to the predictions from that theory, with a sinusoidal displacement with azimuthal wavenumber 2, and displacements up and down coupled to displacements out and in, respectively. The only visible discrepancy is that the angle is not exactly 45°. This discrepancy is probably due to the presence of the free surface and the solid interfaces.

The wavenumber of an unstable disturbance of a vortex ring is also given by Widnall & Tsai (1977). They find that the azimuthal wavenumber, k, can be determined from the relation

$$ka = \kappa \tag{4.1}$$

where a is the vortex core diameter and $\kappa = 2.5$ is a constant. This implies that the wavelength of an instability on a vortex ring is a fixed number of core radii, independent of ring radius. The growth rate is determined from the ratio of core radius to ring radius, and increases with decreasing core radius.

In making the analogy between a vortex ring and the HZ, we assume the vortex core radius to be the height of the zone, which implies that the critical wavenumber would scale with the aspect ratio of the zone. For a zone with aspect ratio 1, (4.1) would predict an azimuthal wavenumber of 2, in agreement with our findings. We have not yet made a complete study of the influence of aspect ratio on the wavenumber selection. But for a zone with aspect ratio 1/3 the most unstable wavenumber was found to be 1, in agreement with (4.1), which gives the prediction 0.84.

It is extremely interesting to note that in the experimental study of Preisser *et al.* (1983) a relation strikingly similar to (4.1) was found. The experiments were done with a fluid with $Pr = 7$. The critical wavenumber after the bifurcation was observed for different aspect ratios. The relation between wavenumber and aspect ratio was found to be

$$k\Lambda^{-1} = 2.2 \tag{4.2}$$

which is quite close to that predicted by Widnall & Tsai (1977), (4.1). It must be pointed out that the transition was in this case not to a steady state but to an

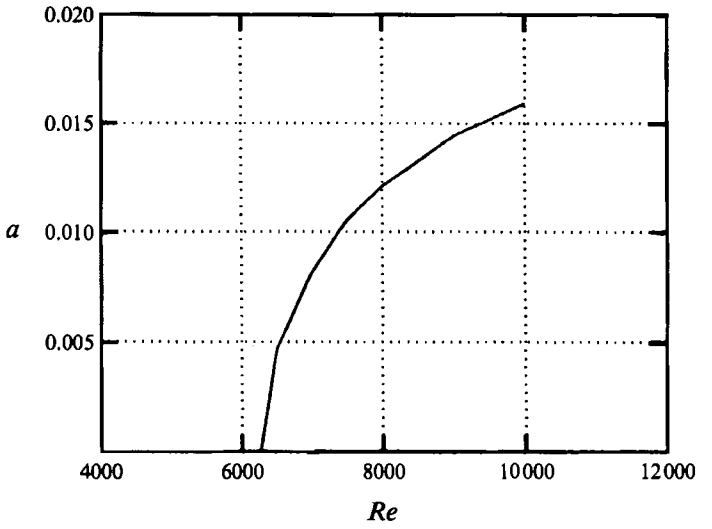

FIGURE 7. Amplitude of the bifurcated solution, $Pr = 0.01, A = 1$.

oscillatory one. This may be due to the fact that the Prandtl number in their study was several orders of magnitude larger than in the present work, and that thermocapillary forces were probably significant in the bifurcated solution.

The azimuthal wavenumber for the stationary solution that we obtain is in agreement with the findings of Rupp *et al.* (1989) who also predict a wavenumber 2-solution for small Prandtl numbers and a similar aspect ratio. They do not present a critical Reynolds number for this bifurcation. The critical Reynolds number and the azimuthal wavenumber obtained in their study do not agree with the results presented in the paper of Kuhlmann & Rath (1993) who predict a wavenumber-1 solution and a much smaller critical Reynolds number than obtained by us. As noted in the introduction an error in their computation was discovered after the publication of their paper. After this error was detected they have made some new computations which are in good agreement with the results presented here (Kuhlmann, private communication 1994).

Ben Hadid & Roux (1990) and Villers & Platten found a transition to a steady multicellular state in two-dimensional rectangular containers, which may at first seem similar to that found here. However, the instability here is intrinsically three-dimensional, being caused by the motion that the curved vortex induces on itself. The closest corresponding situation in a rectangular container would be an initially straight vortex which became wavy along its length, something that could not have been captured in the two-dimensional studies by Ben Hadid & Roux (1990), and Villers & Platten (1992). Also, since we have only studied aspect ratio 1, and the cells observed by Ben Hadid & Roux (1990), and Villers & Platten (1992) have a similar aspect ratio, it is quite unlikely that they would be observed in the present case. It is of course possible that a multicellular state could appear in a longer cylindrical zone, but that would then be a different phenomenon than that discussed above.

4.3. *The second bifurcation: oscillatory state*

Increasing the Reynolds number further will cause the flow to become oscillatory. For a liquid with Prandtl number of 0.01 the critical Reynolds number for this bifurcation

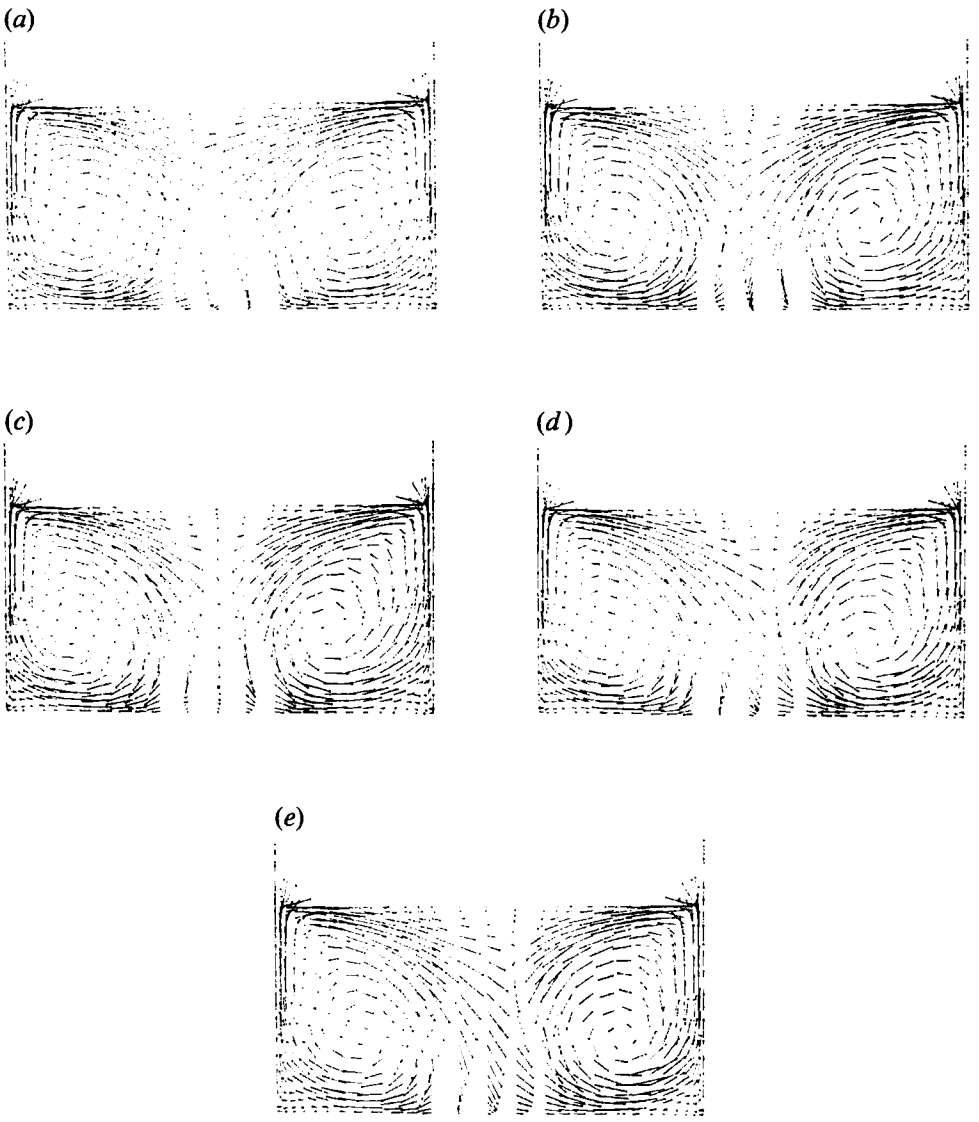

FIGURE 8. Velocity at $\varphi = \pm\pi/2$, (*a–e*) $t = 0, 60, 120, 180, 240$; $Re = 9000, Pr = 0.01$.

was found to be $Re = 6250$. In figure 7 the amplitude of the temperature oscillations at mid-distance between the hot and cold interface can be seen as a function of Reynolds number. The simulations were started with initial data from both higher and lower Reynolds numbers in order to check for any hysteresis. It was not possible to detect any hysteresis and we thus conclude that the bifurcation is supercritical. The amplitude of the bifurcated solution is proportional to $(Re - Re_c)^{1/2}$ as would be expected.

Before giving a description of the oscillatory state it is fruitful to make some comments on the differences between the small Prandtl number case studied in this work and the works performed for Prandtl numbers larger than 1. In the larger Prandtl number case the flow visualizations done in experiments, Preisser *et al.*

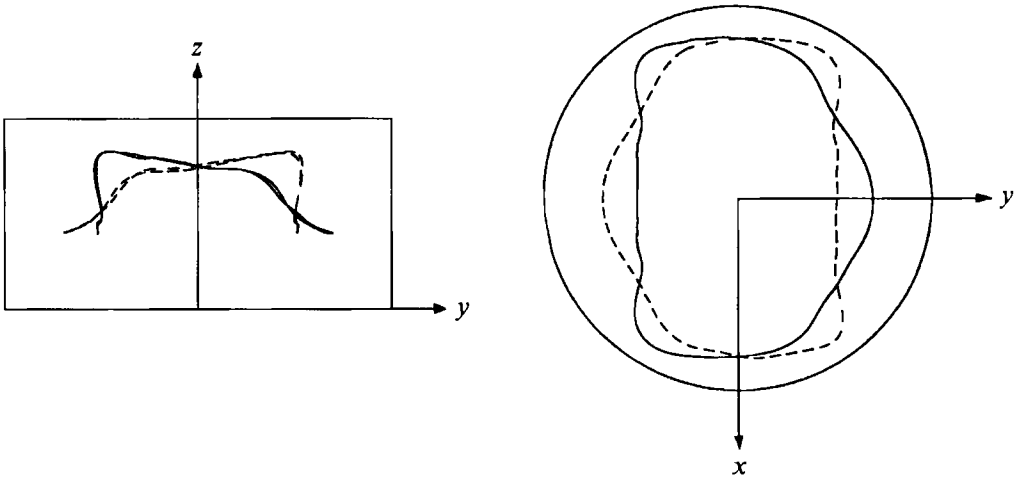

FIGURE 9. Position of the vortex core at two different times in two different planes, $Re = 9000, Pr = 0.01$.

(1983), show that the transition to oscillatory motion occurs directly from a steady axisymmetric state. The time-dependent motion was in these cases described as a three-dimensional travelling wave in the azimuthal direction. For smaller Prandtl numbers on the other hand, the results presented in the previous section show that the flow first becomes steady and non-axisymmetric before it starts to oscillate. This implies that the oscillatory motion for small Prandtl numbers can not be expected to behave like a travelling wave, since the motion after the supercritical bifurcation to an oscillatory state must be a small-amplitude disturbance superimposed on the steady three-dimensional state, if the Reynolds number is sufficiently close to the critical one. Exactly this behaviour was observed in the simulations, and shows that the onset of oscillations is indeed a secondary instability of the steady three-dimensional motion. This rules out the possibility of looking at the oscillatory state as a rotation of the saddle-shaped vortex which would correspond to a travelling wave type of solution similar to those that appear for larger Prandtl numbers.

Snapshots of the velocity field at five different times are presented in figure 8. The velocity field is presented in an r–z cut at $\varphi = \pm\pi/2$ corresponding to the place were the saddle-shaped vortex core has its minimum z value. As can be seen in this figure the flow field oscillates from left to right and back again.

To give a better presentation of how the oscillatory state behaves, the position of the vortex core can be seen in figure 9 in a (y, z)-plane at two different times and in an (x, y)-plane at the same time levels. The bottom segments of the vortex at $\varphi = \pm\pi/2$ move back and forth in the radial direction, roughly keeping the distance between the two positions constant. The upper segments of the vortex core, $\varphi = 0, \pi$, remain at approximately the same postion during the oscillations, but the slope changes, as can be seen in figure 9.

To see if the mechanism causing this oscillatory transition is dependent on an interaction between the temperature and velocity field the Prandtl number was set to zero. For this case a completely similar transition occurred at a Reynolds number of 5962. The oscillations behave in a completely similar fashion as for $Pr = 0.01$. It is thus clearly demonstrated that the oscillatory instability is a pure hydrodynamical

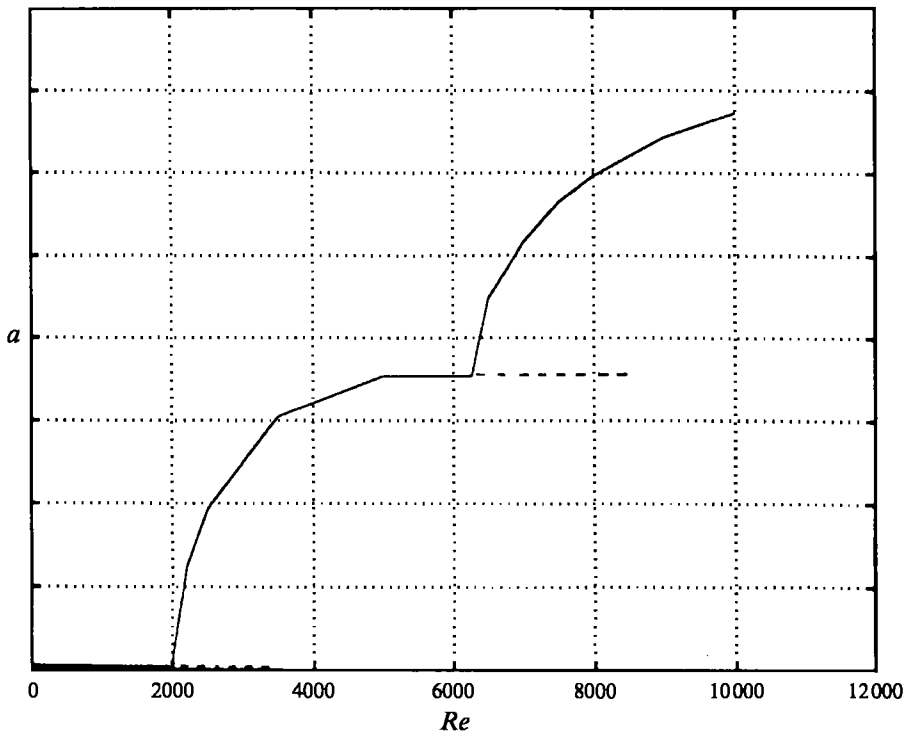

FIGURE 10. Complete bifurcation diagram, $Pr = 0.01, A = 1$.

effect not relying on any thermocapillary mechanism. The oscillatory instability is a secondary instability from the highly three-dimensional steady saddle-shaped vortex state described in the previous section. In the range of Prandtl numbers studied here, relevant for molten semiconductors, the influence of convection on the temperature field is so small that it can be neglected for the transition to oscillatory convection.

There have not been many detailed experimental predictions of the onset of time-dependent motion for liquids with small Prandtl numbers. Cröll, Müller-Sebert & Nitsche (1989) tried to measure the critical Reynolds numbers for a silicon floating zone. They measured a critical Reynolds number for time-dependent motion to be in the range 6100–8700, which agrees quite well with the present study. The experimental setup in that study is, however, quite different from that of a HZ but it is still interesting to see that the critical Reynolds number is close to that predicted by the present results.

5. Conclusions

The stability of the thermocapillary flow in a HZ has been analysed for small Prandtl numbers. When keeping the aspect ratio fixed at 1 and varying the Reynolds number the flow first loses stability to a steady three-dimensional state. This transition can be interpreted in terms of the stability of vortex rings. This analogy gives an understanding of the mechanism behind the instability and it also explains how the azimuthal wavenumber after the bifurcation is selected. In this steady state the azimuthal flow causes an azimuthal temperature gradient. The thermocapillary effect

acts in the opposite direction to the flow and consequently tries to suppress the azimuthal flow. For small Prandtl numbers this suppression is weak.

Increasing the Reynolds number further causes the flow field to become oscillatory. This occurs at a Reynolds number close to 6250 for a Prandtl number of 0.01. This secondary instability is again caused by a purely hydrodynamical effect as demonstrated by the fact that the same instability occurs for a liquid with zero Prandtl number.

The results show that for small Prandtl numbers the route from a steady axisymmetric state via a steady three-dimensional state to an oscillatory three-dimensional state, as the Reynolds number is increased, can be viewed as a succession of purely hydrodynamical instabilities. At small Prandtl numbers the coupling between the temperature and velocity field is so weak that it is of no importance for the instabilities. The complete picture of the different branches for $Pr = 0.01$ can be seen in figure 10. This scenario is independent of the Prandtl number, in the range of Prandtl numbers studied here, $Pr = 0 \rightarrow 0.01$.

The mechanism for transition to oscillatory convection in the HZ is hydrodynamical for small Prandtl numbers. This is in contrast to the higher Prandtl number case, mostly studied experimentally, where the coupling between the temperature and velocity field is probably of crucial importance. It is thus clearly incorrect to draw conclusions about the onset of oscillations from high Prandtl number experiments, and apply these to real crystal growth situations where Pr is small.

The results imply that the flow in the FZ crystal growth process would be non axisymmetric at a much lower Reynolds number than that for oscillations to occur. This non-axisymmetry should be possible to detect in an experiment. If the oscillatory convection is to be avoided in a real crystal growth situation the Reynolds number must be kept below 6250. This is a low value and it might be difficult to achieve such a small Reynolds number, at least for large to moderate sized zones.

REFERENCES

BEN HADID, H. B. & ROUX, B. 1990 Thermocapillary convection in long horizontal layers of low-Prandtl-number melts subject to a horizontal temperature gradient. *J. Fluid Mech.* **221**, 77–103.

CHANG, C. E. & WILCOX, W. R. 1976 Analysis of surface tension driven flow in floating zone melting. *Intl J. Heat Mass Transfer* **19**, 355–356.

CRÖLL, A., MÜLLER-SEBERT, W. & NITSCHE, R. 1989 The critical Marangoni number for the onset of time-dependent convection in silicon. *Materials Res. Bull.* **24**, 995–1004.

GOLUB, G. H. & LOAN, C. F. VAN 1989 *Matrix Computations.* The John Hopkins University Press.

HANSBO, P. & SZEPESSY, A. 1990 A velocity pressure streamline diffusion finite element method for the incompressible Navier-Stokes equations. *Computer Meth. Appl. Mech. Engng* **84**, 175–192.

KAZARINOFF, N. D. & WILKOWSKI, J. S. 1989 A numerical study of marangoni flows in zone-refined silicon crystals. *Phys. Fluids* A **1**, 625–627.

KAZARINOFF, N. D. & WILKOWSKI, J. S. 1990 Bifurcations of numerically simulated thermocapillary flows in axially symmetric float zones. *Phys. Fluids* A **2**, 1797–1807.

KUHLMANN, H. C. & RATH, H. J. 1993 Hydrodynamic instabilities in cylindrical thermocapillary liquid bridges. *J. Fluid Mech.* **247**, 247–274.

NEITZEL, G. P., CHANG, K. T., JANKOWSKI, D. F.& MITTELMANN, H. D. 1993 Linear stability theory of thermocapillary convection in a model of the float-zone crystal-growth process. *Phys. Fluids* A **5**, 108–114.

NEITZEL, G. P., LAW, C. C., JANKOWSKI, D. F. & MITTELMANN, H. D. 1991 Energy stability of thermocapillary convection in a model of the float-zone crystal-growth process. ii: Nonaxisymmetric disturbances. *Phys. Fluids* A **3**, 2841–2846.

PREISSER, F., SCHWABE, D. & SCHARMANN, A. 1983 Steady and oscillatory thermocapillary convection in liquid columns with free cylindrical surface. *J. Fluid Mech.* **126**, 545–567.

RUPP, R., MÜLLER, G. & NEUMANN, G. 1989 Three-dimensional time dependent modelling of the marangoni convection in zone melting configurations for gas. *J. Cryst. Growth* **97**, 34–41.

SHEN, Y., NEITZEL, G. P., JANKOWSKI, D. F. & MITTELMANN, H. D. 1990 Energy stability of thermocapillary convection in a model of the float-zone crystal-growth process. *J. Fluid Mech.* **217**, 639–660.

SHIEN, J. 1993 A remark on the projection-3 method. *Intl J. Numer. Meth. Fluids* **16**, 249–253.

SMITH, M. K. 1986 Instabilities mechanisms in dynamic thermocapillary liquid layers. *Phys. Fluids* **29**, 3182–3186.

SMITH, M. K. 1988 The nonlinear stability of dynamic thermocapillary liquid layers. *J. Fluid Mech.* **194**, 391–415.

SMITH, M. K. & DAVIS, S. H. 1983*a* Instabilities of dynamic thermocapillary liquid layers. Part 1. convective instabilities. *J. Fluid Mech.* **132**, 119–144.

SMITH, M. K. & DAVIS, S. H. 1983*b* Instabilities of dynamic thermocapillary liquid layers. Part 2. surface-wave instabilities. *J. Fluid Mech.* **132**, 145–162.

VILLERS, D. & PLATTEN, J. K. 1992 Coupled buoyancy and marangoni convection in acetone: experiments and comparison with numerical simulations. *J. Fluid Mech.* **234**, 487–510.

WIDNALL, S. & TSAI, C.-Y. 1977 The instability of the thin vortex ring of constant vorticity. *Proc. R. Soc. Lond.* A **287**, 273–305.

XU, J.-J. & DAVIS, S. H. 1983 Liquid bridges with thermocapillarity. *Phys. Fluids* **26**, 2880–2886.

XU, J.-J. & DAVIS, S. H. 1984 Convective thermocapillary instabilities in liquid bridges. *Phys. Fluids* **27**, 1102–1107.

ZEBIB, A., HOMSY, G. & MEIBURG, E. 1985 High marangoni number convection in a square cavity. *Phys. Fluids* **28**, 3467–3476.